Supplementary Information

Characterizing Friction for Fiber Reinforced Composites Manufacturing: Method Development and Effect of Process Parameters

Arit Das[1,2], Gabriel Y.H. Choong[3], David A. Dillard[2,4], Davide S.A. De Focatiis[3,*], Michael J. Bortner[1,2,*]

[1]Department of Chemical Engineering, Virginia Tech, Blacksburg, VA 24061
[2]Macromolecules Innovation Institute, Virginia Tech, Blacksburg, VA 24061
[3]Department of Mechanical, Materials and Manufacturing Engineering, University of Nottingham, Nottingham, NG7 2RD, UK
[4]Department of Biomedical Engineering and Mechanics, Virginia Tech, Blacksburg, VA 24061

*Co-corresponding authors: Dr. Davide De Focatiis (email: Davide.Defocatiis@nottingham.ac.uk) and Dr. Michael J. Bortner (email: mbortner@vt.edu)

Table S1: List of angular velocities and normal forces required to maintain constant mean sliding velocity and constant contact pressure on the prepreg sample, as dictated by Equations 1 and 2, while varying the annular width of the ring geometry.

Ring outer diameter (mm)	Annular width (mm)	Contact area (mm^2)	Normal force (N)	Angular velocity (mrad/s)	Mean linear velocity (mm/s)	Contact pressure (kPa)
25	0	490.6	32.5	14.4	120.1	66.4
	1	75.4	5.0	10.0		
	2	144.4	9.6	10.4		
	4	263.8	17.5	11.3		

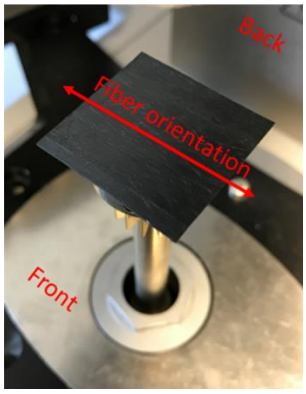

Figure S1: The orientation of the fibers of the composite prepreg with respect to the rheometer during a typical frictional sliding experiment.

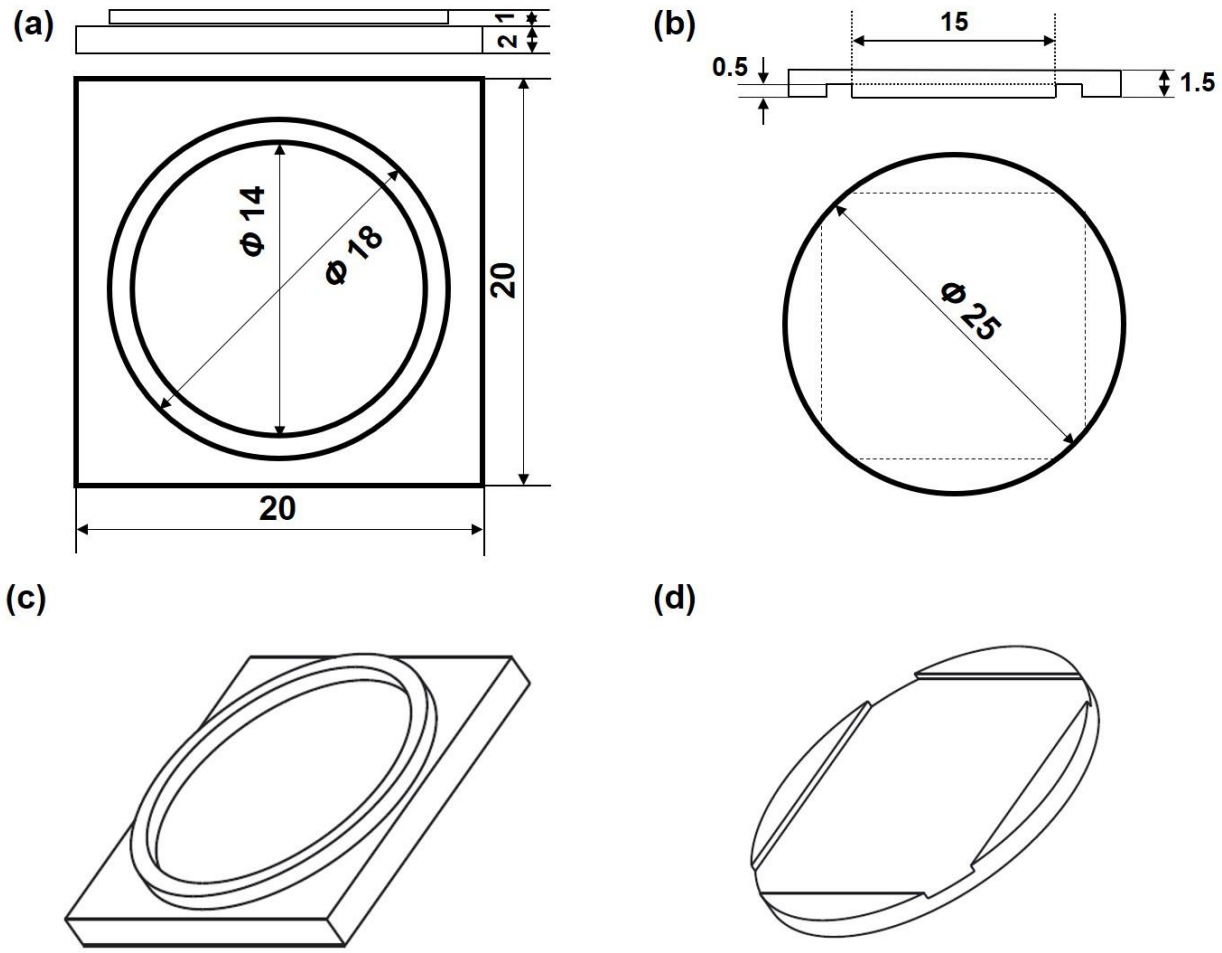

Figure S2: (a) Schematic of the acrylic fixture used for the imaging experiments along with the relevant dimensions in mm; (b) schematic of the plate used to accommodate the acrylic fixture along with the relevant dimensions in mm; (c) isometric view of the part of the acrylic fixture that contacts the prepreg; (d) isometric view of the modified top-plate for the rheometer that locates the square part of the acrylic fixture.

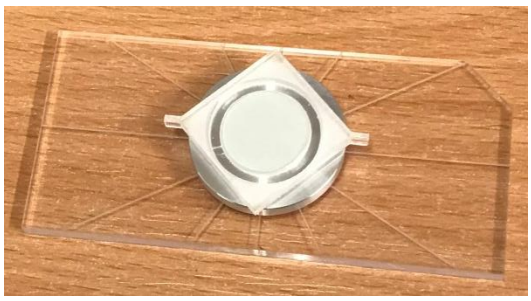

Figure S3: The locating fixture used to image the prepreg using optical microscopy. The prepreg was imaged through the transparent annular region of the smaller acrylic fixture.

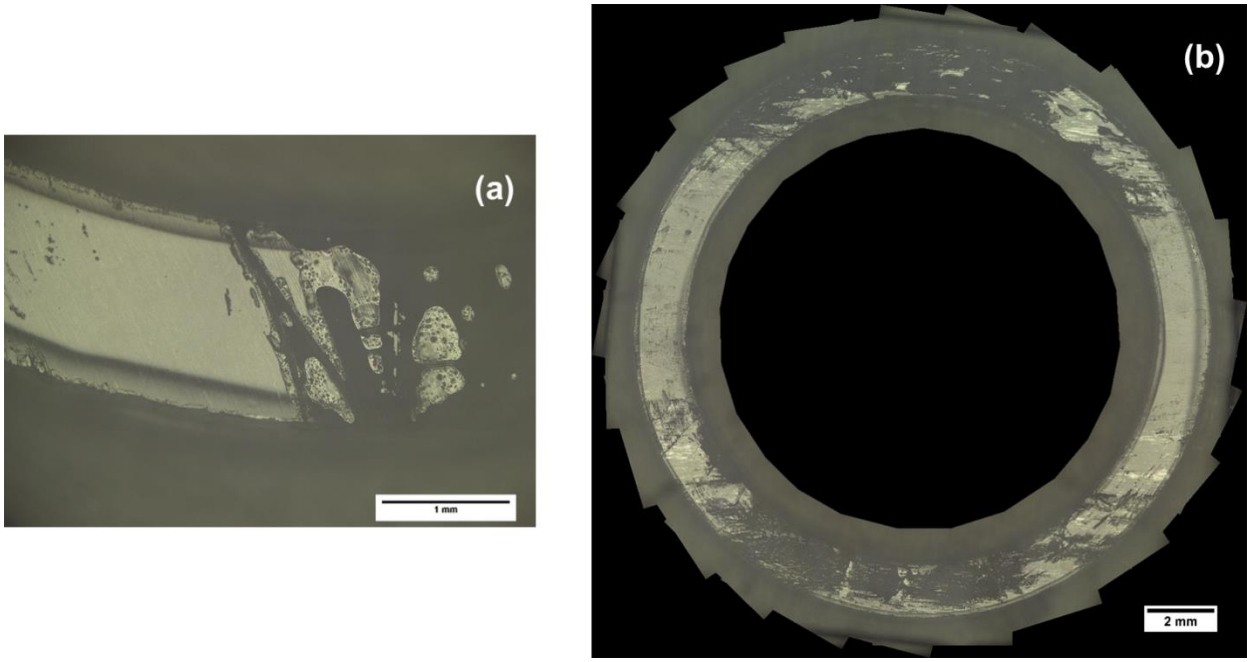

Figure S4: (a) Representative image of the optical micrographs obtained during imaging the prepreg surface through the annulus of the acrylic fixture; (b) The composite image obtained by stitching 25 individual images using Microsoft ICE software; this image was post-processed to calculate contact area as discussed in Section 4.2 of the manuscript.

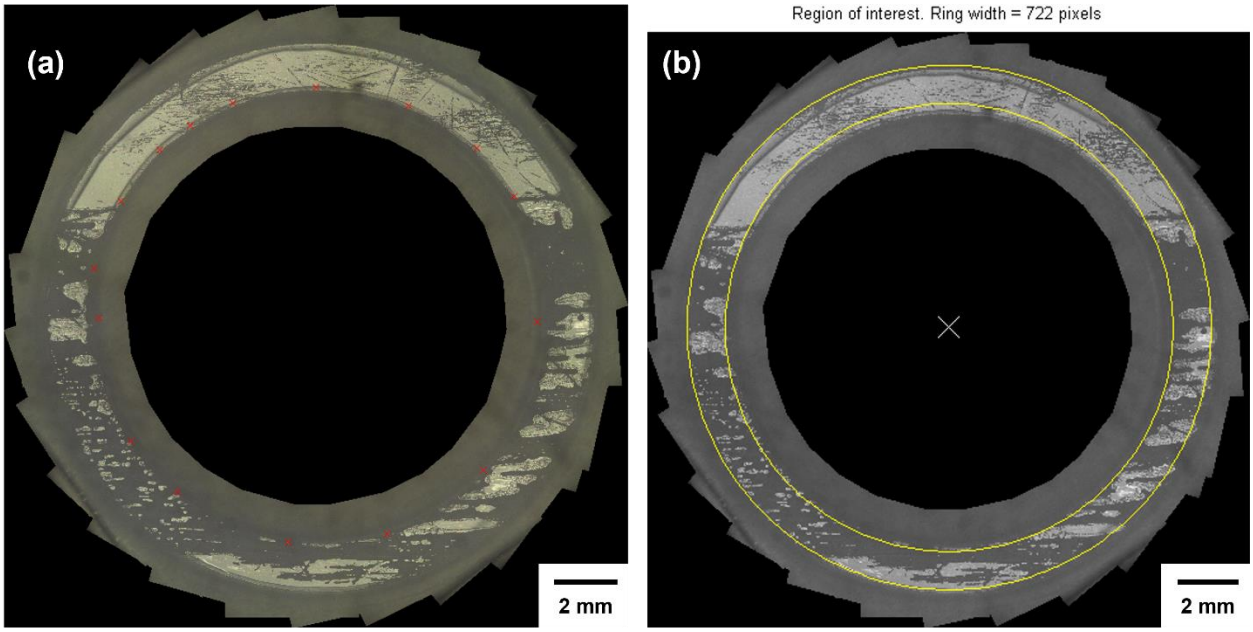

Figure S5: (a) The composite image imported to MATLAB; the red dots indicate the user-defined points on the inner circumference which is used to create the outer circumference and locate the center of the image; (b) Region of interest (outlined in yellow) of the composite image that is subsequently analyzed to evaluate contact area between the prepreg and the acrylic

fixture. The cross-mark in middle of the image indicates the center coordinates. The region of interest for all the composite images analyzed comprised of 722 pixels.

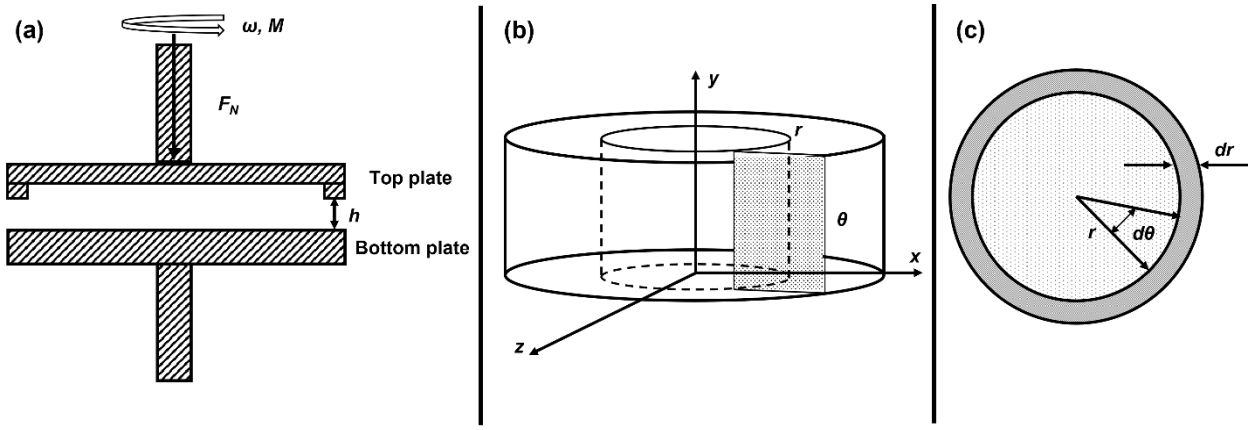

Figure S6: (a) Schematic of the annular parallel plate rheometer setup employed in this study; (b) representative side view of the rheometer with the annular plate geometry; and (c) differential area element used for calculating the torque measured by the rheometer during the sliding frictional test procedures.

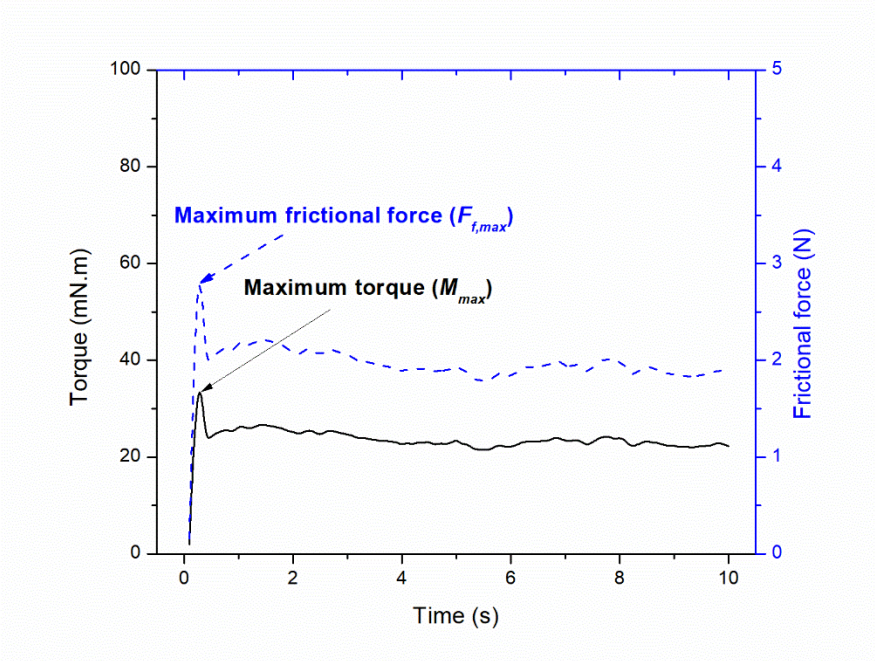

Figure S7: Representative torque (black) and frictional force (blue) profiles as a function of sliding time during a typical frictional sliding experiments using a 25 mm parallel plate with an annulus having a width of 1 mm.

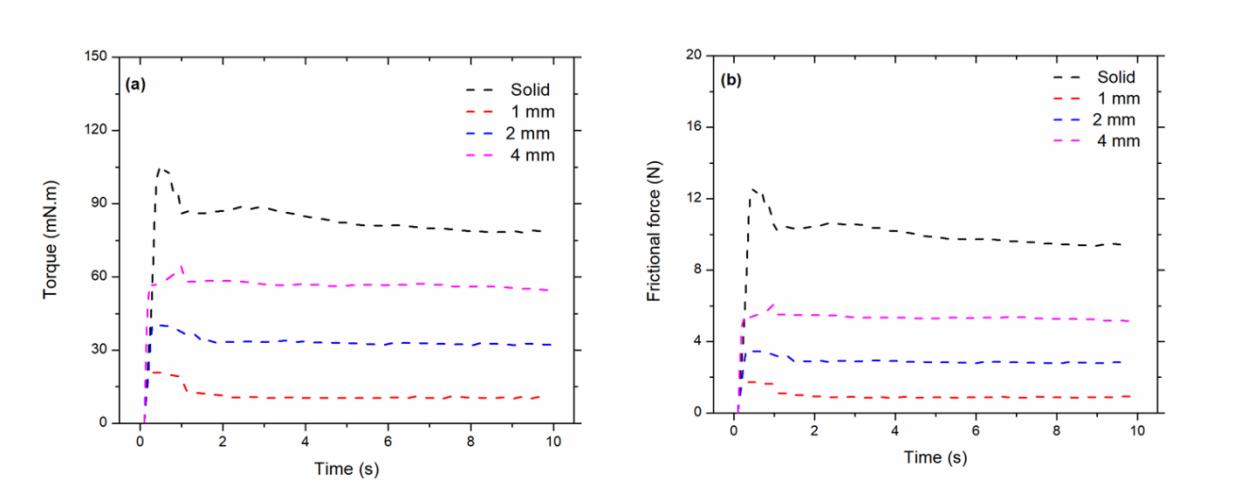

Figure S8: (a) Torque and (b) frictional force evolution with time during frictional sliding experiments performed at 40°C using 25 mm parallel plates of varying widths (1 mm, 2 mm, 4 mm, and solid plate). The experimental conditions for the different geometries are presented in Table S1.

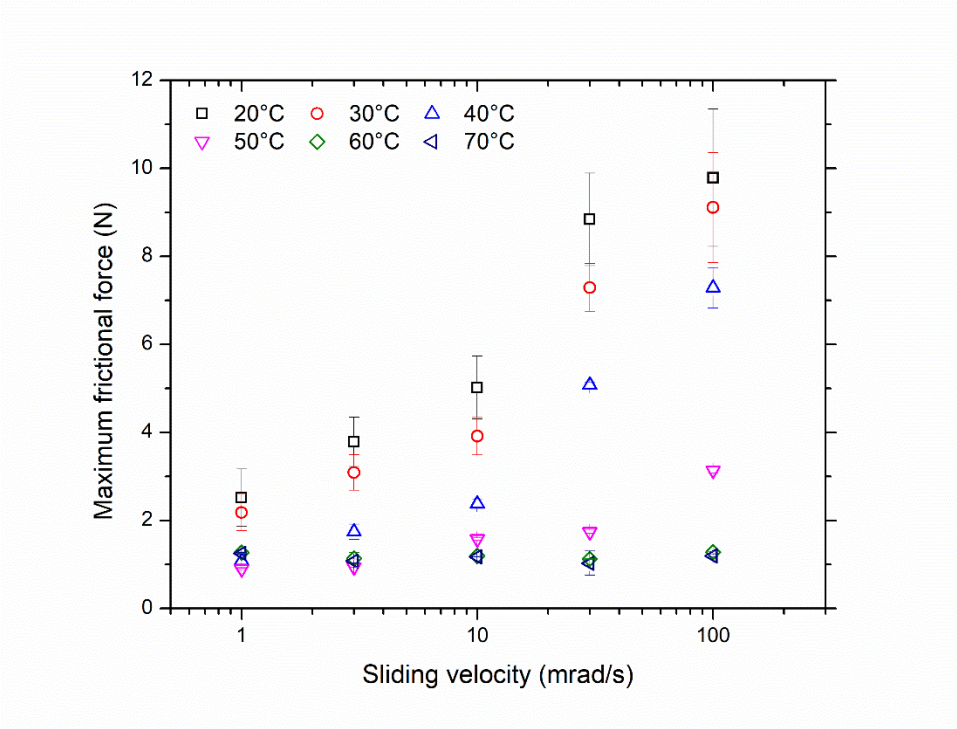

Figure S9: Effect of angular sliding velocity on the maximum frictional force recorded during the sliding experiments performed using 25 mm parallel plates with 1 mm width at different temperatures under a constant normal force of 5 N.

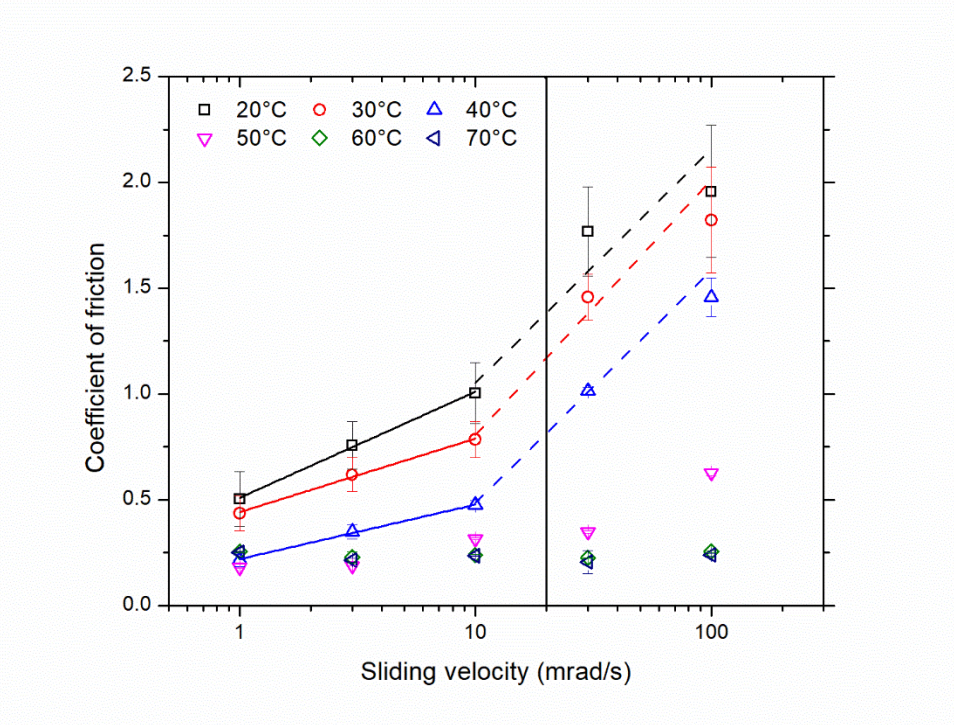

Figure S10: Variation in the coefficient of friction as a function of sliding velocities at different temperatures obtained from frictional sliding experiments performed at 5N normal force. The solid and dashed lines (to highlight the change in slope of the plot) represent the linear fits to the data using Equation 16 of the manuscript for the 1-10 and 10-100 mrad/s regions, respectively.

Table S2: Values of friction parameter (*C*), friction index (*n*), and normalized friction factor (*R*) obtained by non-linear fitting of Equation 16 to the data obtained from the frictional sliding experiments performed at different normal forces in the temperature range of 30-50°C under 10 mrad/s angular velocity.

Temperature (°C)	C (Pa^{1-n})	n	R (Pa^{1-n})	R^2 (fit)
30	1.89 ± 0.01	0.455 ± 0.007	4.154	0.999
40	0.864 ± 0.01	0.629 ± 0.011	1.373	0.999
50	0.401 ± 0.006	0.868 ± 0. 019	0.462	0.999

Table S3: Values of power-law constant (μ_0) and power law exponent (m) obtained by non-linear fitting of $\mu = \mu_0 F_N^m$ to the data obtained from the frictional sliding experiments performed at different normal forces in the temperature range of 30-50°C under 10 mrad/s angular velocity.

Temperature (°C)	μ_0	m	R^2 (fit)
30	1.89 ± 0.02	-0.544 ± 0.007	0.999
40	0.86 ± 0.01	-0.370 ± 0.011	0.996
50	0.40 ± 0.01	-0.131 ± 0.019	0.953

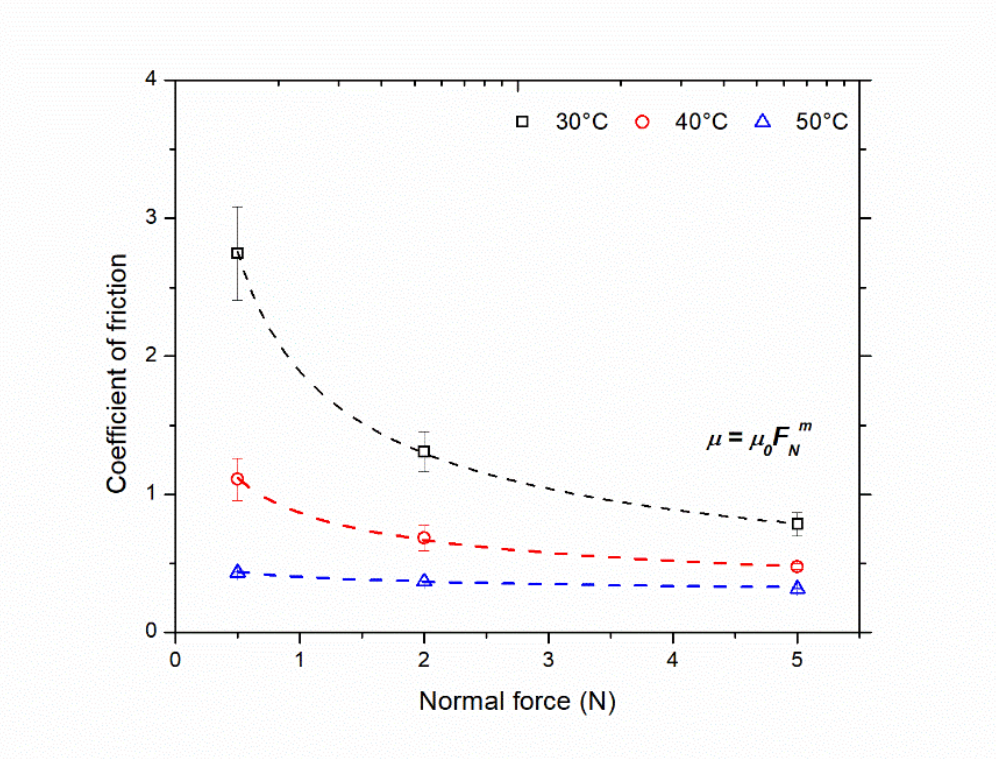

Figure S11: Variation in the coefficient of friction as a function of applied normal force at different temperatures obtained from frictional sliding experiments performed at 10 mrad/s. The dashed lines represent the non-linear fits to the data using the power law equation $\mu = \mu_0 F_N^m$.

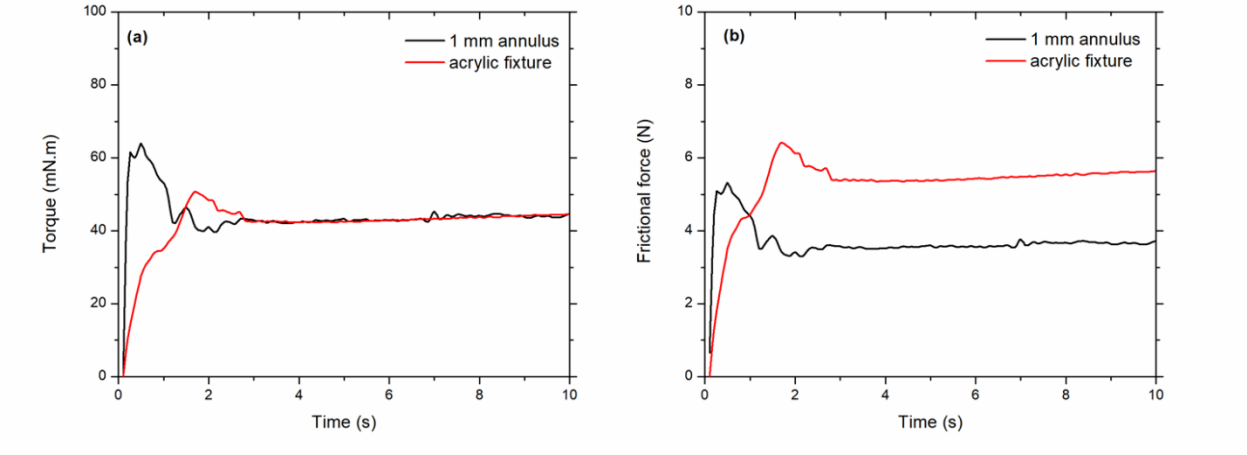

Figure S12: (a) Torque and (b) frictional force variations with sliding time for the two different geometries (25 mm parallel plate with 1 mm width and the acrylic fixture used for imaging) obtained from the frictional sliding experiments performed at room temperature while maintaining constant contact pressure and constant mean linear sliding velocity.

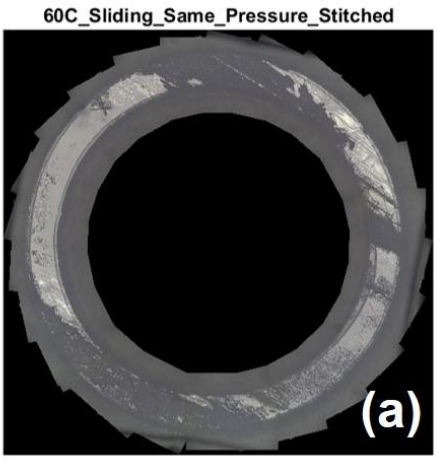
60C_Sliding_Same_Pressure_Stitched
(a)

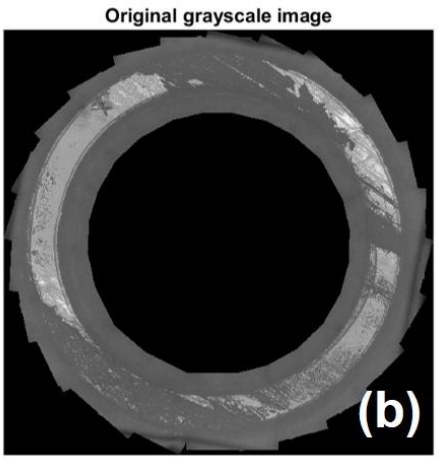
Original grayscale image
(b)

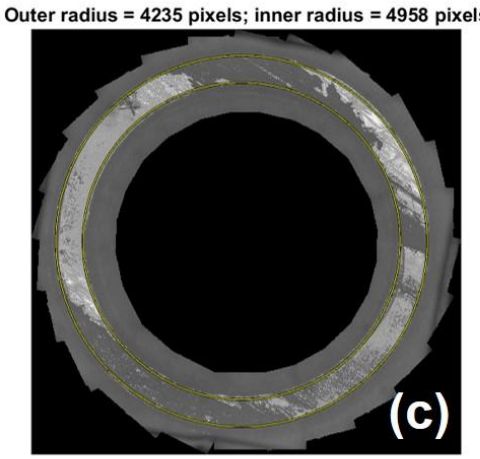
Outer radius = 4235 pixels; inner radius = 4958 pixels
(c)

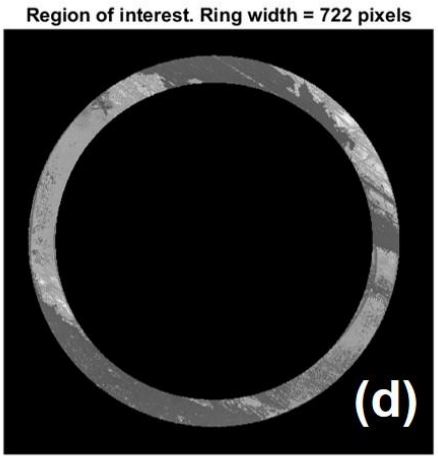
Region of interest. Ring width = 722 pixels
(d)

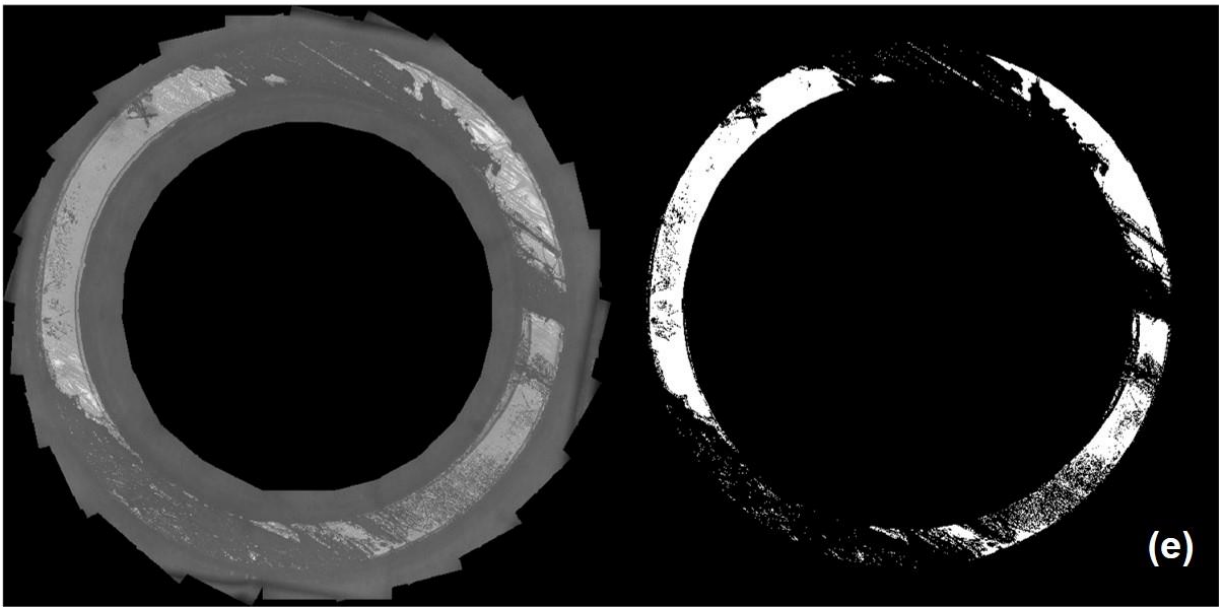
(e)

Figure S13: Snapshots from the different stages of the image processing procedure for calculating contact area (a) original composite image; (b) composite image converted to grayscale; (c) determination of inner and outer radii of acrylic fixture on the prepreg surface; (d) generating the mask and region of interest from the grayscale composite image; (e) comparison between the original image and image analyzed for contact area calculation after implementing a proper thresholding algorithm (Isodata). The relative ratio of the number of black pixels and total number of pixels within the region of interest is used to calculate the contact area of the manuscript.